

AD-A268 248



## TATION PAGE

Form Approved  
OMB No. 0704-0188

1. To average 1 hour per revision, including the time for reviewing instructions, searching existing data sources, gathering the collection of information, send comments regarding this burden estimate or any other aspect of this form, its instructions, and its instructions, to Washington Headquarters Services, Directorate for Information Operations and Reports, 1215 Jefferson Ave., Washington, DC 20540-6001, Washington, DC 20540-6001.

DATE

3. REPORT TYPE AND DATES COVERED

Final 15 Jan 91 - 14 Jan 92

## 4. TITLE AND

On the Simultaneous Measurements of Two Velocity Components  
in the Turbulent Spot

## 5. FUNDING NUMBERS

AFOSR - 91 - 0134

2307/BS

## 6. AUTHOR(S)

A. Seifert, M. Zilberman and I. Wygnanski

## 7. PERFORMING ORGANIZATION NAME(S) AND ADDRESS(ES)

Department of Fluid Mechanics and heat Transfer  
Faculty of Engineering, Tel Aviv University,  
Ramat-Aviv, Israel 66978

8. PERFORMING ORGANIZATION  
REPORT NUMBER

AFOSR TR- 93 0618

## 9. SPONSORING / MONITORING AGENCY NAME(S) AND ADDRESS(ES)

DTIC  
ELECTE  
AUG 18 1993

AFOSR/NA  
Building 410  
Bolling AFB,  
Washington DC 20332-6448

10. SPONSORING / MONITORING  
AGENCY REPORT NUMBER

AFOSR-91-0134

## 11. SUPPLEMENTARY NOTES

## 12a. DISTRIBUTION / AVAILABILITY STATEMENT

This document has been approved  
for public release and sale; its  
distribution is unlimited.

93 8 17 018

## 12b. DISTRIBUTION STATEMENT

93-19124



22 P8

## 13. ABSTRACT (Maximum 200 words)

Measurements of spanwise and streamwise velocity components in a turbulent spot artificially initiated in a Blasius boundary layer are described. A special hot-wire rake consisting of 8 "V" arrays was built for this purpose. The data reveals the existence of a strong spanwise component of velocity which attains its maximum value at the tip of the spot and is centered around an elevation equivalent to the displacement thickness of the unperturbed boundary layer. This perturbation velocity resembles a wave which follows the leading interface of the spot and may therefore be amenable to analysis.

## 14. SUBJECT TERMS

Boundary-layer, transition, hot-wire anemometry

## 15. NUMBER OF PAGES

23

## 16. PRICE CODE

17. SECURITY CLASSIFICATION  
OF ABSTRACT

unclassified

18. SECURITY CLASSIFICATION  
OF THIS PAGE

unclassified

19. SECURITY CLASSIFICATION  
OF ABSTRACT

unclassified

## 20. LIMITATION OF ABSTRACT

**ON THE SIMULTANEOUS MEASUREMENTS OF TWO VELOCITY COMPONENTS  
IN THE TURBULENT SPOT**

**By**

**A. Seifert, M. Zilberman and I. Wygnanski**

Department of Fluid Mechanics and heat Transfer  
Faculty of Engineering,  
Tel Aviv University,  
Ramat-Aviv, Israel 66978

Accession For	
NTIS CRA&I	<input checked="" type="checkbox"/>
DTIC TAB	<input type="checkbox"/>
Unannounced	<input type="checkbox"/>
Justification	
By	
Distribution /	
Availability Codes	
Dist	Avail and/or Spec
A-1	

DTIC QUALITY INSPECTED 3

**ABSTRACT**

Measurements of spanwise and streamwise velocity components in a turbulent spot artificially initiated in a Blasius boundary layer are described. A special hot-wire rake consisting of 8 "V" arrays was built for this purpose. The data reveals the existence of a strong spanwise component of velocity which attains its maximum value at the tip of the spot and is centered around an elevation equivalent to the displacement thickness of the unperturbed boundary layer. This perturbation velocity resembles a wave which follows the leading interface of the spot and may therefore be amenable to analysis.

## INTRODUCTION

There is abundance of evidence suggesting that the interior structure of a transitional spot embedded in a Blasius boundary layer is similar to a fully developed turbulent boundary layer. Thus, the manner in which the turbulent spot destabilizes the surrounding vortical fluid is of interest to those attempting to delay transition as well as those interested in the structure and control of the turbulent boundary layer. The spot spreads in the spanwise and streamwise directions at an incredible rate in the absence of favourable streamwise pressure gradient. Since the fluid within the laminar boundary layer surrounding the spot is already vortical, the propagation of the spot-interface near the solid surface may be achieved by destabilizing the flow surrounding the spot. The destabilization process is enhanced when the surrounding boundary layer is unstable to small disturbances of the Tollmien -Schlichting type. In this case two, oblique wave packets, trailing the spot amplify and break down to generate new turbulent spots which soon coalesce with the "parent" spot<sup>1,2</sup>. Such wave packets are absent when the surrounding boundary layer is stable<sup>3</sup> and their absence is associated with diminishing the rate of spread of the spot. The absence of breakdown to turbulence near the trailing interface of the spot affects the shape of the trailing interface changing the plan-view of the spot from its typical "arrow head" (or heart like) shape to a triangular shape with the trailing interface perpendicular to the direction of streaming. However, despite the stable surroundings, the spot keeps spreading in a manner which is only vaguely understood.

In an attempt to correlate the internal structure of the spot with its rate of spread and formulating the latter within the context of the classical stability theory it was decided to measure carefully the lateral component of velocity associated with the passage of the spot. A special hot-wire rake was built for this purpose and the principal results of the investigation are reported in this manuscript. The free stream velocity was maintained at 11.4m/sec throughout the experiment and the measurements were made at  $6.65 \cdot 10^5 \leq Re_x \leq 10.2 \cdot 10^5$  based on the distance measured from the leading edge of the plate. Very detailed measurements were made near the tip of the spot (i.e. at  $80\text{mm} \leq Z \leq 96\text{mm}$ .) at the first measuring station. this data was acquired at 10 elevations from the plate varying between  $0.5 < Y/\delta_{\text{laminar}}^* < 3$ . Special attention was paid to the regions in which the velocity gradients were high.

### SOME NOVEL EXPERIMENTAL PROCEDURES

Since the experimental apparatus, data acquisition and reduction techniques are described in earlier papers<sup>4,2</sup>. The reader is therefore directed to those sources for additional information. A photograph of the 16-wire "V" probe used in this experiment is shown in figure 1. The Z resolution of each V array is approximately 1.7mm. and the average distance between adjacent centers of the V arrays is 2.3mm. Consequently, simultaneous two-component velocity data is provided by this rake over an aggregate span of 16.04 mm corresponding to the distance between the centers of the first and the last V array in the rake. The rake was mounted on a traversing mechanism having 6 degrees of freedom corresponding to translation in the X,Y,Z directions and rotation around all three axes. Translation in the Y direction and rotation around the Y axis were computer controlled because the rake had to be moved out of the boundary layer to be calibrated in yaw. The maximum resolution provided by the stepper motor was 12.7 microns in Y and 0.3° in yaw. Manual rotation around the X and Z axes enabled one to align the rake parallel to the plate and normal to the direction of streaming.

Yaw and speed calibration was made by using "look-up" tables of 4096 (corresponding to the 12 bit resolution of the analog-to-digital converter) points per wire. The experiment was conducted at a free stream velocity of  $U_{\infty} = 11.4\text{m/sec.}$  and therefore the velocity calibration carried out between 1.5m/sec. and 12m/sec. This range was subdivided into 7 segments and a fourth order polynomial was fitted to the data. The accuracy of the velocity calibration was within 1% of  $U_{\infty}$ . Since the hot-wires in each V array were inclined to the rake axis by 45°, yaw calibration was restricted to  $\pm 33^\circ$  only and was done at 6° interval. The restriction on the yaw angle provided a limitation on the minimum distance from the surface at which measurements could be done. The streamwise and spanwise velocity components were obtained from a pair of voltages recorded simultaneously by each wire ( $E_1$  and  $E_2$ ) in the "V" array (figure2). It was required that the measured voltages were within the calibration range during the passage of the spot. The hot-wire calibration was tested for drift and if found acceptable the rake was moved to the measuring station in the boundary layer. Final alignment of the rake was done in laminar flow where the local velocity was  $0.3U_{\infty}$ . Two conditions were imposed on each V-array at this location:

- (i) that the velocity gradient around this location was linear and the extrapolated distance to the wall measured by all the arrays was approximately equal.

- (ii) that the spanwise component of velocity measured by each array was sufficiently small so that the inclination angle measured did not exceed  $2^\circ$ .

All these requirements could be met, under normal operating conditions, provided the nominal distance of the rake from the wall was 1mm. or larger. The sampling frequency was 4KHz. per channel and the number of events recorded varied between 400 to 600. The larger number of events was recorded near the wall because the data processing was too slow to make the transformation from voltage to velocity in real time. Thus the calibration range might have been exceeded in some of the events; when this was detected during the "off-line" processing of the data those events were discarded and reduced the pool of data available for ensemble-averaging. Whenever the rake elevation was reduced below 1mm., in the range of X locations considered, 30%-50% of the events were lost in this manner.

### DISCUSSION OF RESULTS

Ensemble averaged, streamwise velocity perturbation contours recorded during the passage of the spot are plotted in figure 3. These data were plotted in the (Z, T) plane at an approximate elevation above the surface which is equivalent to the displacement thickness of the unperturbed, laminar boundary layer (i.e. at  $\delta^* \approx 1$ ). The measurements presented were made at 3 streamwise locations: 60; 75; & 90cm. downstream of the spark generator or 90; 105; & 120cm. downstream of the leading edge of the plate. The perturbation contour levels observed vary from -3% to +11% and are plotted at intervals of 2%. The negative velocity perturbation regions are hatched. The dimensional spanwise distance is marked on the left of each figure while the time elapsed from the initiation of the spot by the spark is marked on top. The corresponding dimensionless times and spanwise distances are marked at the bottom and right side of each figure. The average location of the interface determined by the intermittency factor<sup>2</sup>  $\gamma = 0.5$  is also shown in figures 3 & 4.

There is a steep positive gradient in the streamwise velocity component (figure 3) following the leading edge of the spot at the first two streamwise locations (i.e. at  $X_s = 60$  and 75 cms.). There is a region of negative velocity perturbation beyond the tip of the spot (i.e. at  $Z/X_s > 0.15$ ) at all streamwise locations measured. At  $X_s = 90$  cms. the negative velocity perturbation extends from the tip of the spot to its plane of symmetry (i.e. to  $Z = 0$ ). The

continuous region of negative velocity perturbation under the "overhang" of the leading interface was never shown although it could have been inferred from the data presented in reference 4. Closer to the solid surface there is only a positive velocity perturbation<sup>2</sup>. It suggests that the initial breakdown to turbulence is associated with an ejection of low velocity fluid from the surface outward (see figure 11a of reference 7) before the effective turbulent mixing enhances the velocity near the surface. It is quite possible that the reason for not seeing this at smaller  $X_s$  distances stems from the short duration of the event relative to the jitter in the time of arrival of the spot but it may also be a phenomenon which evolves whenever the spot attains some form of equilibrium. The negative velocity perturbation region follows the leading interface so precisely that the two occurrences are probably interconnected. The high velocity region following the spot, or the "calmed" region in the parlance of Schubauer and Klebanoff<sup>5</sup>, exceeds in length the turbulent length of the spot at all  $Z$  locations. The wave packets following the spot are also observed at all three streamwise locations shown. The number of wave-crests in the packet increases with  $X_s$ , while the distance separating the first wave-crest from the trailing interface of the spot did not change between  $X_s = 60\text{cms.}$  and  $X_s = 90\text{cms.}$  The ensemble averaged amplitudes have diminished at  $X_s = 90\text{cms.}$  because of partial breakdown to turbulence. In fact a 20% intermittency factor contour was measured between  $2.2 < (U_\infty T/X_s) < 2.6$  centered around  $Z/X_s = 0.08$ . These results are in qualitative agreement with the data presented in reference 2 at  $Y/\delta^* \approx 0.6$ .

The corresponding  $W$ - perturbation contours are plotted in figure 4 for the identical locations discussed above. The contour levels plotted vary between  $-0.5\%$  and  $+4.5\%$  at intervals of  $1\%$  where the positive sign implies outward direction from the plane of symmetry. It is interesting to note that the maximum outward (positive) velocity measured at  $Y/\delta^* \approx 1$  is located inside the turbulent zone near the leading interface at the tip of the spot. The contours of the cross-flow component follow the leading interface of the spot and are entirely absent from its core, its trailing edge and from the "calmed-flow" regions. The inflow (i.e. negative  $W$ ) contours outside the turbulent zone coincide with an excess of the streamwise velocity. This is seen most clearly in the wave packet region and just prior to the arrival of the spot. Both  $W$  and  $dW/dZ$  essentially vanish near the plane of symmetry<sup>4</sup>.

Conditionally aligned perturbation contours in the  $Y$ - $T$  plane measured near the tip of the spot

(i.e.  $0.137 \leq Z/X_s \leq 0.160$ ) are shown in figures 5 and 6. The velocity perturbations recorded by the rake during the passage of the spot enabled one to detect the instantaneous location of the turbulent interface for each event. The rake was positioned in such a way that the average location of the spot tip occurred at its center. The data was then shifted in the Z direction in order to represent the flow relative to the average location of the interface. The maximum, ensemble averaged cross flow velocity was increased in this manner from  $0.045U_\infty$  shown in figure 4 to  $0.08U_\infty$  (figure 6). Some individual realizations indicated that the maximum spanwise velocity W could be as high as  $0.17U_\infty$  implying that the alignment of the data can still be improved. This is important because the spanwise rate of spread of the spot would become comparable to the average inclination of the velocity vector measured at the tip of the spot to the plane of symmetry.

The excess in the streamwise velocity perturbation near the wall, so prominent in the vicinity of the plane of symmetry<sup>6,7</sup> totally disappears from within the turbulent region at  $Z/X_s \geq 0.145$  (figure 5). Only some wavy remnants of the "calmed region" are observed at this spanwise location, however, the excess velocity under the "overhang" of the leading interface persists to the very tip of the spot (figure 5). The perturbed low speed fluid appears to be transported away from the plane of symmetry by the outward perturbation in W (figure 6). The maximum cross-flow velocity reduced is approximately 8% of  $U_\infty$  at  $Z/X_s \approx 0.13$  and it reduces to 6.5% near the average location of the tip. It was postulated before (reference 2 figure 14) that the waves in the packet might turn in the streamwise direction and coalesce distorting the mean velocity behind the spot and generating the "calmed region". The relatively prominent transverse velocity in the inflow direction following the spot (observed in figure 6 at:  $0.137 < Z/X < 0.160$ ) tend to reinforce this notion.

The ensemble averaged velocity perturbation normal to the surface can be calculated from the rake data by using continuity. Although it is not claimed to be an accurate technique it provides some insight into the structure of the flow. Thus all three components of perturbation velocity corresponding to  $Z/X = 0.137$  are presented in figure 7. A strong upwash (V positive) velocity perturbation equivalent to  $3.5\%U_\infty$  is visible above the leading interface of the spot. The strongest upwash does not coincide with the strongest cross flow or streamwise velocity perturbations, it is also confined to the streamwise extent of the spot while the inwash (the negative W perturbation) and the streamwise velocity perturbations linger for a

long time behind the trailing interface at this Z cross section.

Plotting vector diagrams in the Y-t plane (figure 8) and in the Z-t plane (figure 9) near the outer tip of the spot indicates that the velocity perturbations associated with the passage of the tip of the spot can be represented by vortices. The core of the spanwise vortex is situated below  $Y/\delta^* = 1$  and inboard of  $Z/X_s = 0.140$  (figure 8) while at larger Z the spanwise vorticity perturbation occurs near the surface. The center of the vertical vortex (figure 9) is located near the trailing interface of the tip and its effects are felt beyond  $Z/X_s = 0.160$ . Although velocity vectors give only a qualitative representation of circulation there can be little doubt about the presence of strong perturbation vorticity in this region. These observations are consistent with the presence of single arm of the classical "horse-shoe" or "A" shaped vortex situated near the tip of the spot which is sufficiently coherent to be detected in spite of the averaging process. An intensive search for the second arm of the "horse-shoe" did not yield positive results to date.

Examining the vector diagrams over the entire span of the spot at  $Y/\delta^* = 1$  gives no indication that other "A" vortices exist. The averaged data suggest that a single vortex spanning the spot parallel to its leading edge dominates the transition process. One may even notice a periodicity in the pattern between  $0 < Z/X_s < 0.06$  (figure 10). The period is approximately 13 msec. and it corresponds to the dominant period of the Tollmien Schlichting wave-packet which trails the spot. One may surmise from this information that the breakdown to turbulence occurs along the leading edge of the spot and it may be associated with an instability mechanism. A contour plot of the turbulent intensity (a "true RMS" defined in reference 2) is shown in figure 11 for the data presented in figures 3 and 4. These contours indicate that most of the turbulent activity below the "overhang" is associated with the above mentioned vortex or wave. The intensity gradients near the boundaries can be enhanced by accounting for the intermittency factor of the average time of arrival of the interfaces but the character of the turbulent intensity distribution does not change by the "correction" (see the "corrected" RMS plot shown in figure 11). Since high turbulence intensities are generally observed following transition, these contours may serve as an additional evidence that the leading interface of the spot destabilizes the laminar boundary layer beneath the "overhang".



## CONCLUDING REMARKS

Visual observations of turbulent spots<sup>8-10</sup> reveal that the spot contains a large number of eddies. In fact, provided the Reynolds number is sufficiently high, the structure apparent in the interior of the spot is indistinguishable from the structure of the turbulent boundary layer<sup>8</sup>. Filtered velocity records capturing the entire cross section of a single spot<sup>7</sup> on the plane of symmetry reveal the large number of eddies it contains. Detailed measurements in the "nascent" spot at low Re landed themselves to a reconstruction of the velocity perturbation associated with the most probable event<sup>11</sup>, however the details were lost at higher Re and larger streamwise distances from the origin. It was hoped that the V rake described earlier will have a sufficiently good spatial resolution to reveal the substructure near the tip of the spot. Although this hope did not materialize, the data revealed the significance of the cross-flow component which monotonically increased toward the tip of the spot. It appears that much of the entrained fluid near the plane of symmetry and mid-span of the spot is ejected in the spanwise direction outward. A cross flow component which is non-existent on the laminar flow side of the leading interface near the tip of the spot is very strong on the turbulent side of it (figure 12). The streamwise component of the velocity profile is also distorted between  $1 < Y/\delta^* < 3$  and possesses an inflection point in that region. Both components of the perturbation velocity are unstable and may contribute to a rapid breakdown to turbulence. Improved stability analysis of the flow can now be made. Furthermore, novel methods of data analysis like the wavelet technique may avoid the loss of information associated with conventional statistical methods. The current experiment should be supplemented by either Direct Numerical Simulation (DNS) or Large Eddy Simulation (LES) which will include the possible feedback effect between the spot, the wave packets and the "calmed region". These effects were not considered by Spalart because of the limited resolution of his calculations.

## REFERENCES

1. Wignanski, I., Haritonidis, J.H., and Kaplan, R.E., On a Tollmien-Schlichting wave packet produced by a turbulent spot, *Journal Fluid Mechanics*, (1979), 92, 505-.
2. Glezer, A., Katz, Y., and Wignanski, I., On the breakdown of the wave packet trailing a

turbulent spot in a laminar boundary layer, *Journal Fluid Mechanics*, (1989) 198, pp.1-26.

3 Katz, Y., Seifert, A., and Wygnanski, I., On the evolution of a turbulent spot in a laminar boundary layer in favourable pressure gradient, *Journal Fluid Mechanics*, (1990), 221, 1-22.

4 Wygnanski, I., Sokolov, M., and Friedman, D., On a turbulent spot in a laminar boundary layer, *Journal Fluid Mechanics*, (1976), 78, 785-819.

5 Schubauer, G. B., and Klebanoff, P.S., Contributions to the mechanics of boundary layer transition, NACA Report number 1289, (1956).

6 Zilberman, M., Wygnanski, I., and Kaplan, R.E., , *Physics of Fluids Supplement* 20, S258.

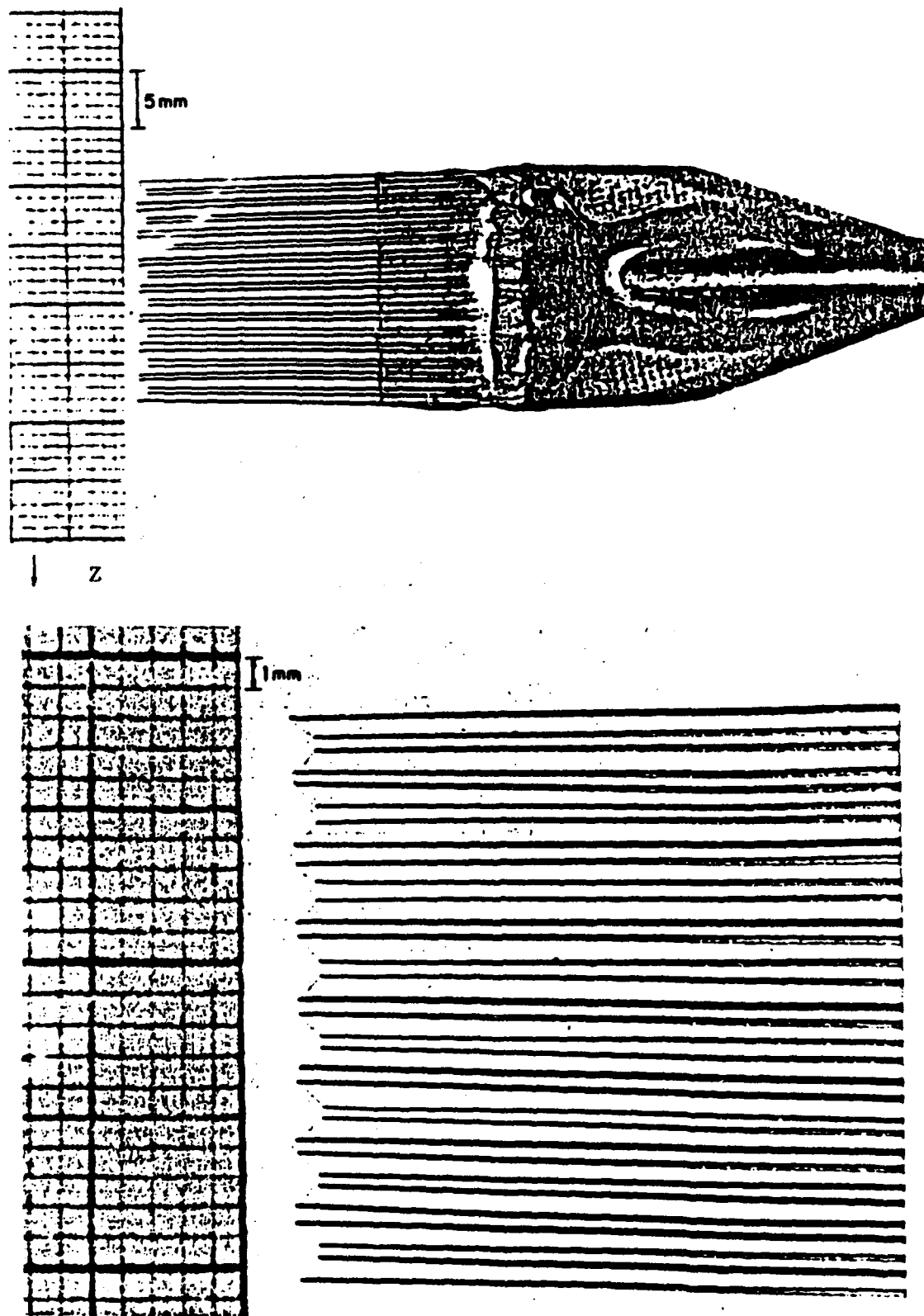
7 Wygnanski, I., Zilberman, M., and Haritonidis, J.H., On the spreading of a turbulent spot in the absence of pressure gradient, *Journal Fluid Mechanics*, (1982), 123, 69-90.

8 Cantwell, B., Coles, D., and Dimotakis, P., Structure and entrainment in the plane of symmetry of a turbulent spot, *Journal Fluid Mechanics*, (1978) 87, 641.

9 Gad -El- Hak, M., Blackwelder, R.F., and Riley, J.J., On the growth of turbulent regions in laminar boundary layers, *Journal Fluid Mechanics*, (1982) 110, pp. 73-.

10 Matsui, T. ...., in: R. Eppler and H. Fasel (eds.) *Laminar - turbulent transition*, Springer Verlag Publishers (1980) pp. 288-

11 Wygnanski, I., On turbulent spots. *Proceedings of the 7th Biennial Symposium on Turbulence - Rolla , Missouri* (1983) pp.390-400.



Hot wire Rake.

Figure 1

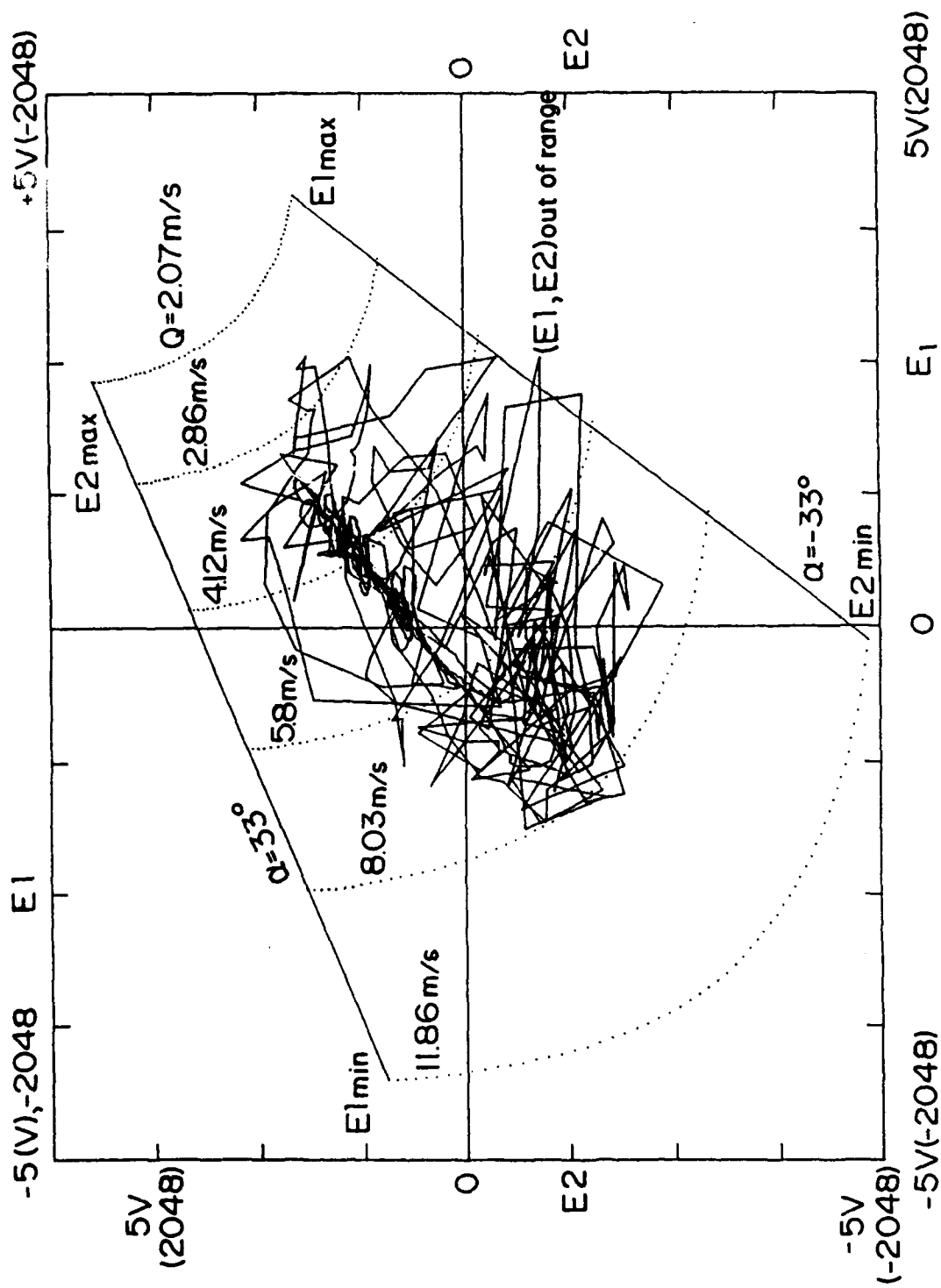


Figure 2

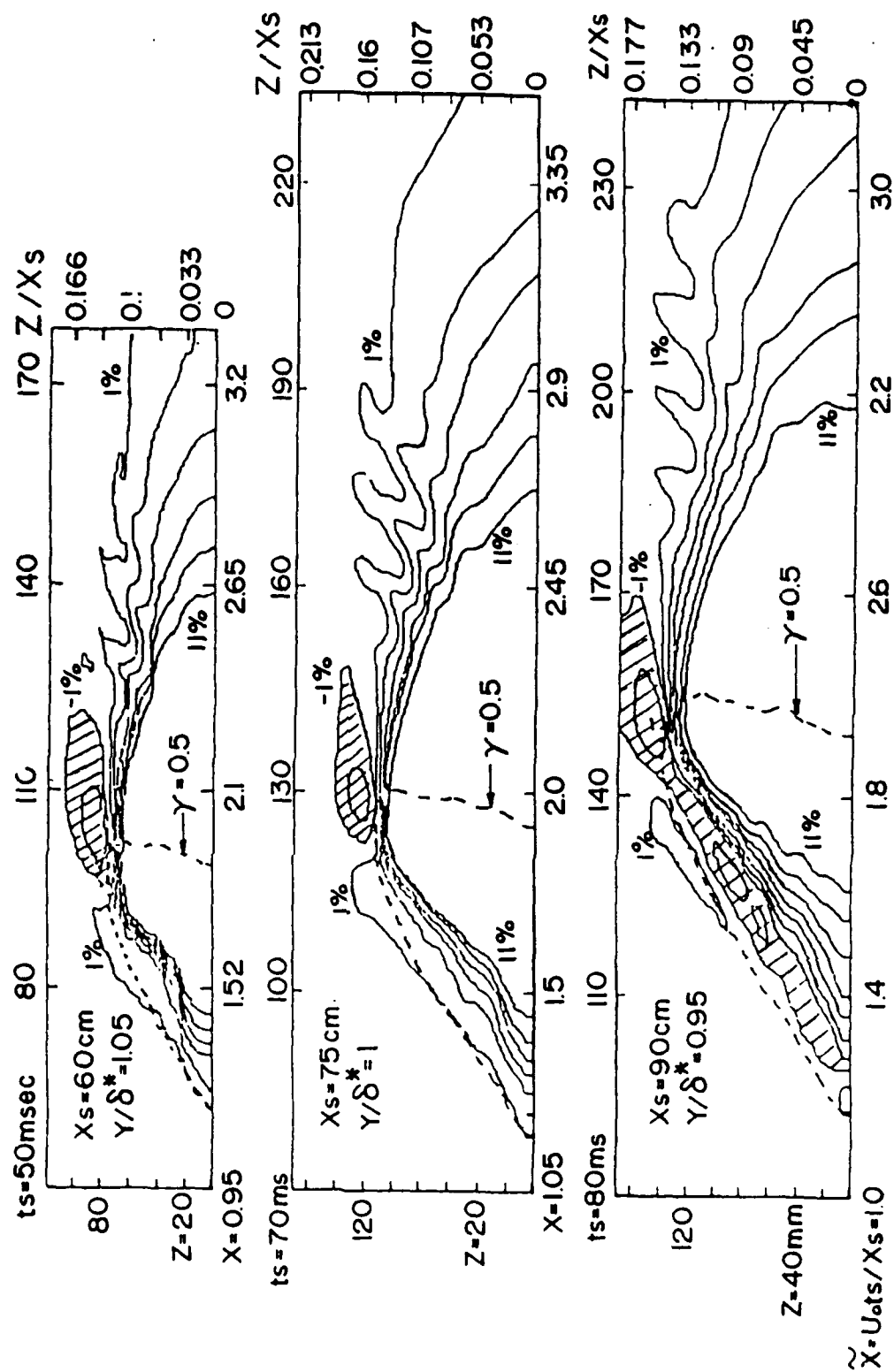


Figure 3

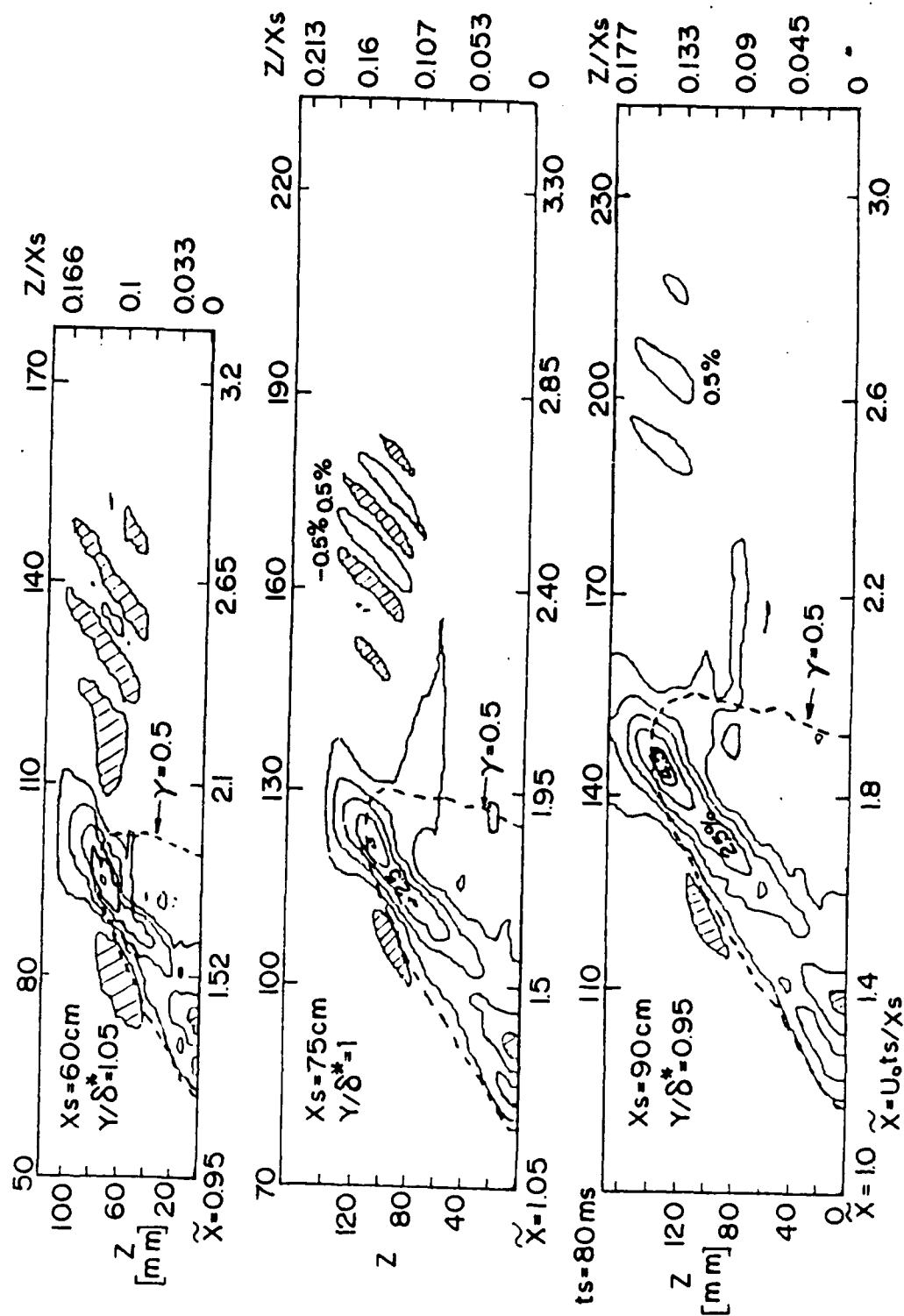


Figure 4

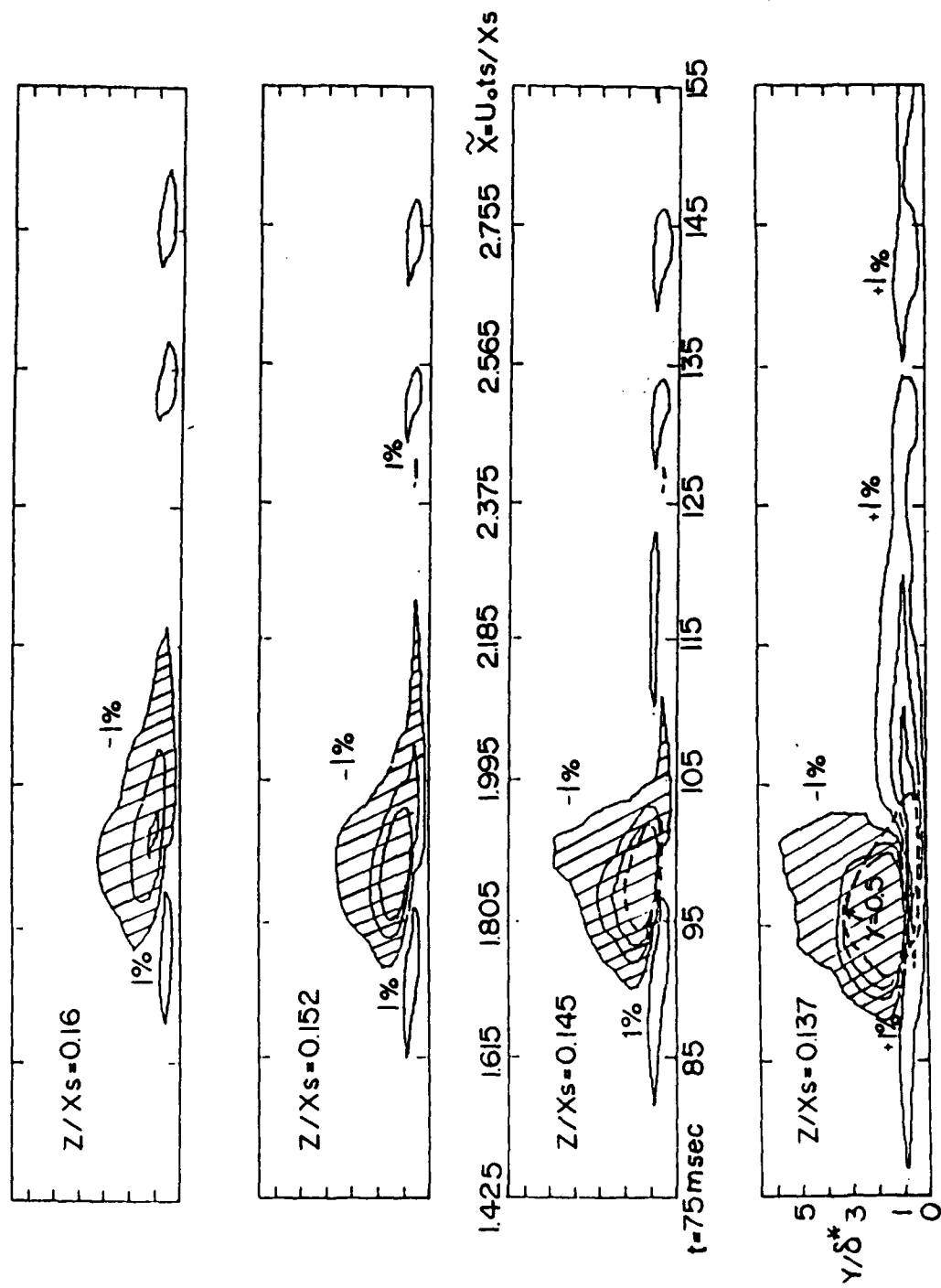


Figure 5

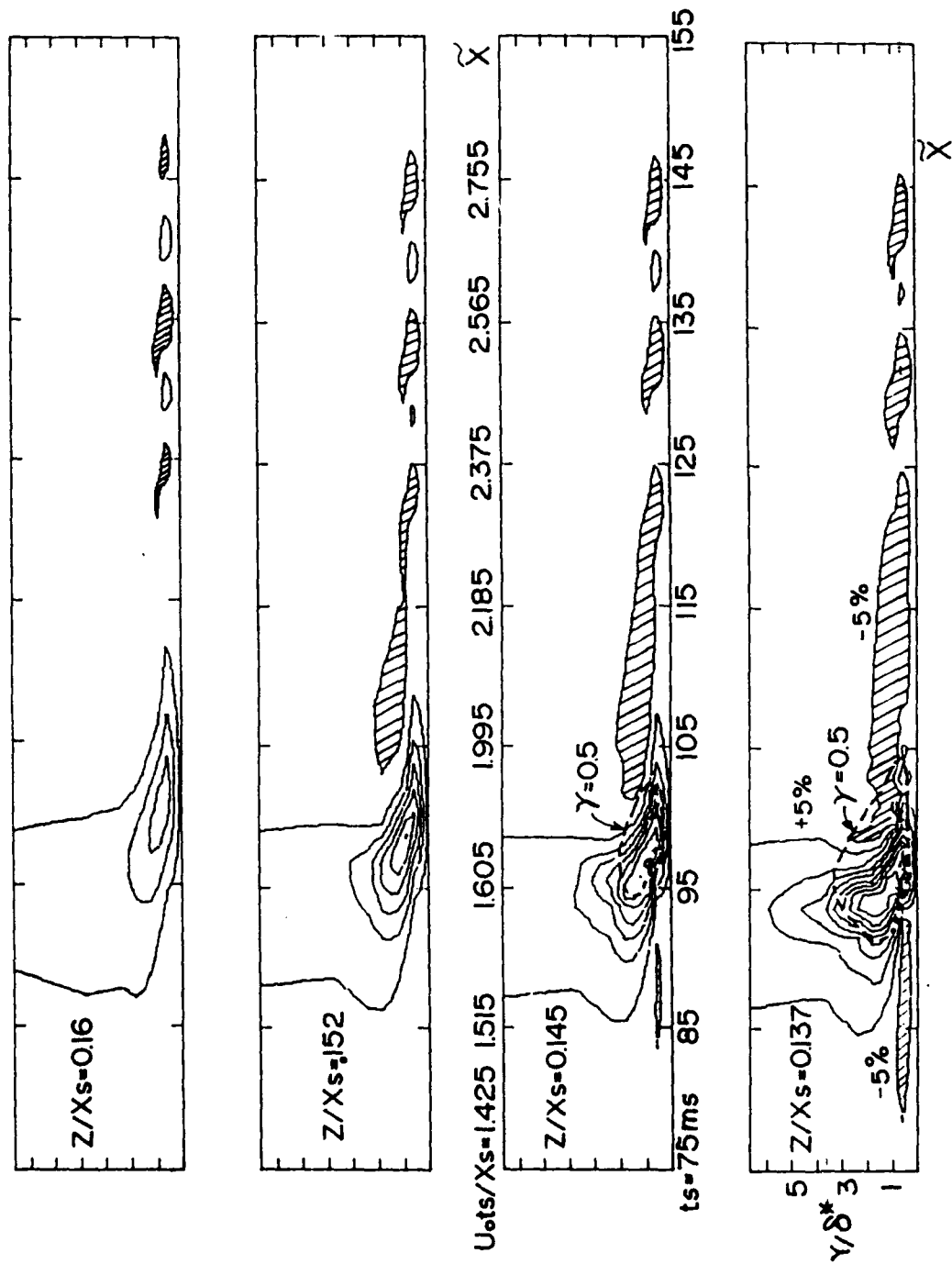
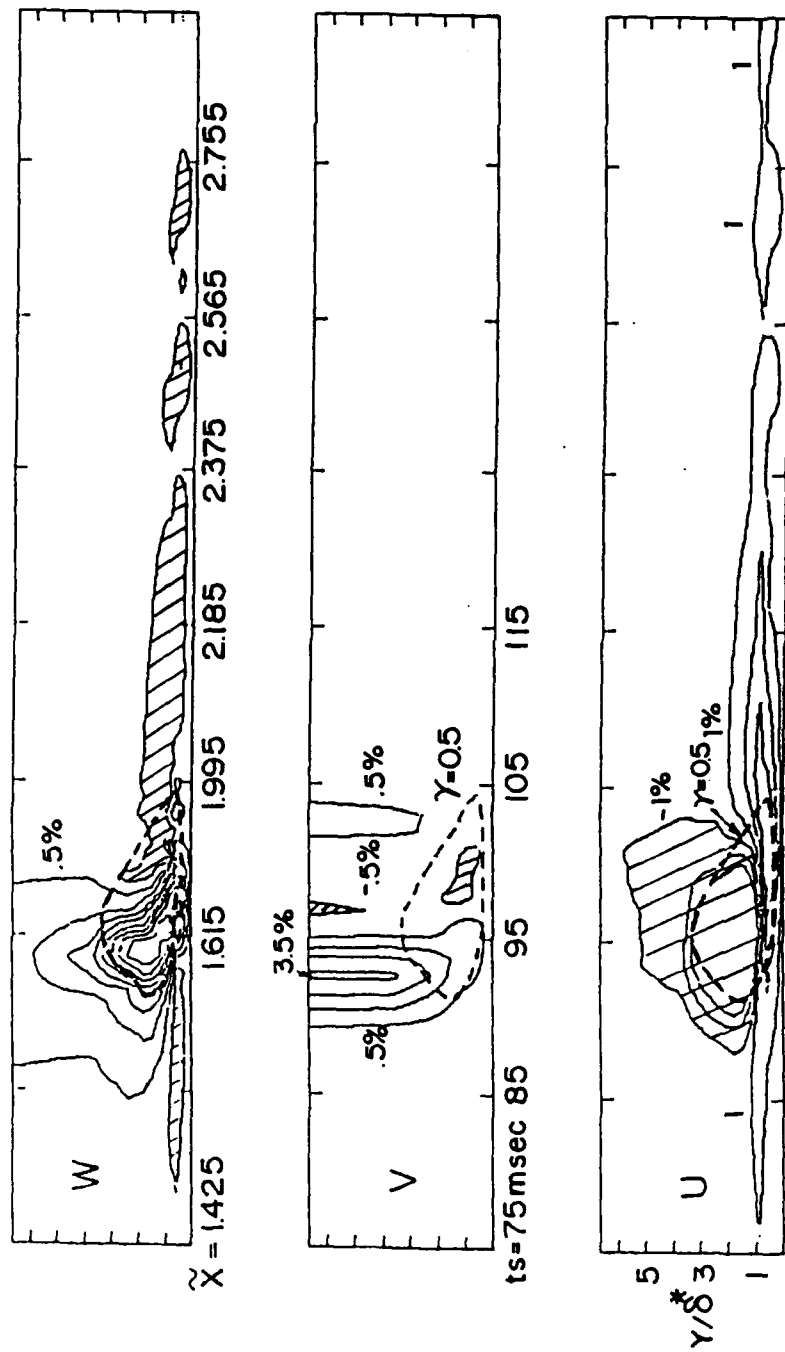


Figure 6





$$\tilde{X} = U_{ots}/X_s$$

Figure 7

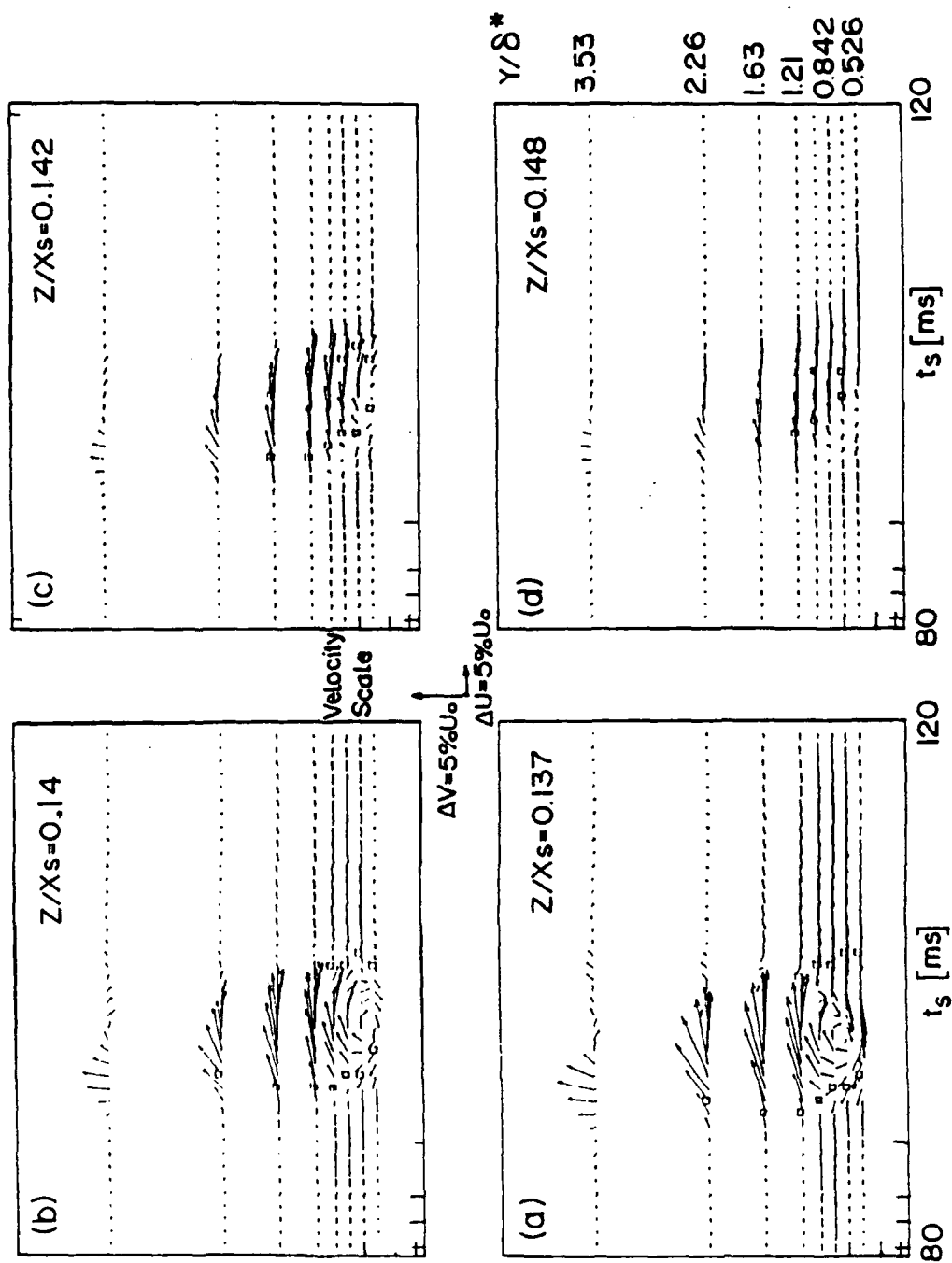


Figure 8

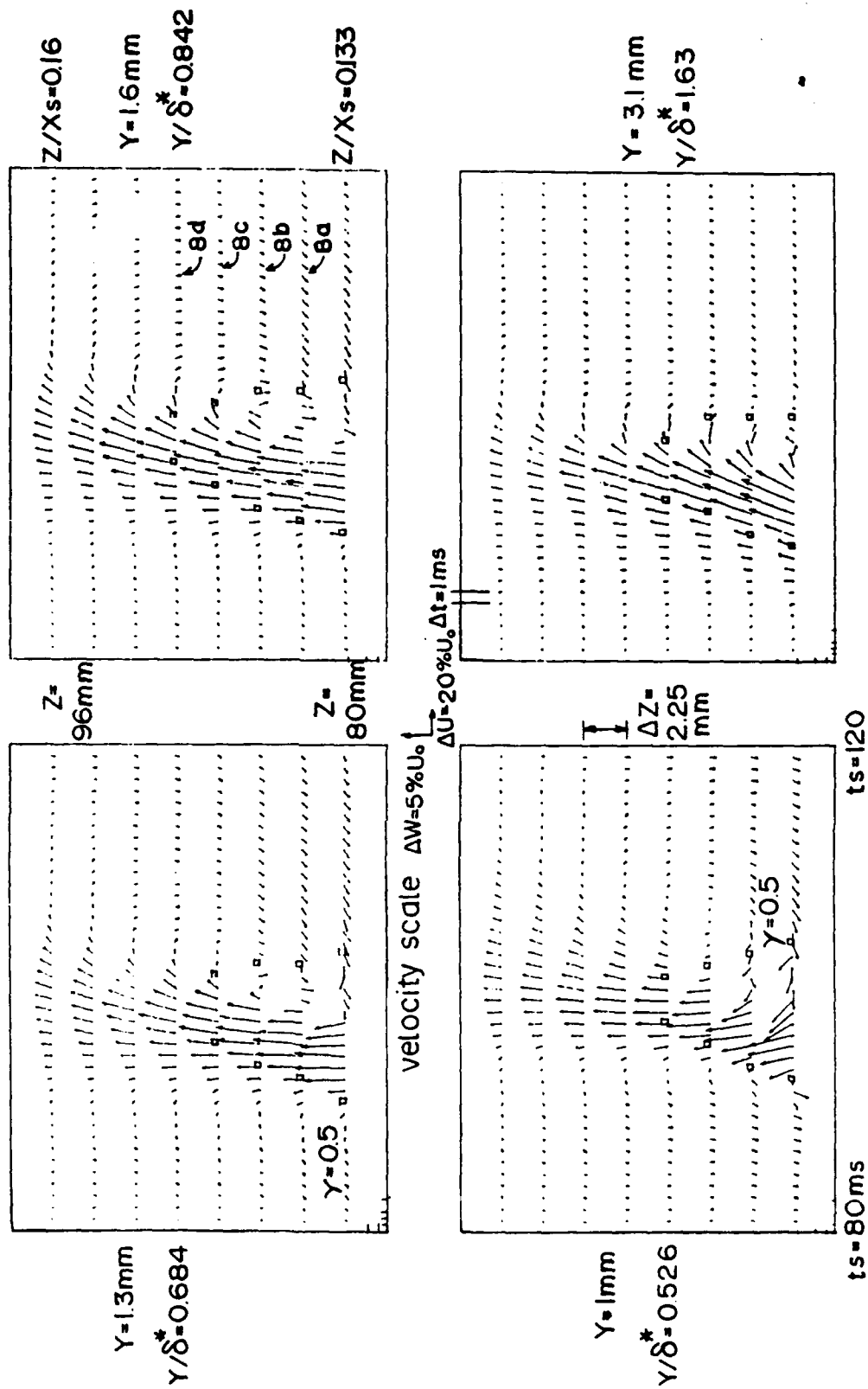


Figure 9

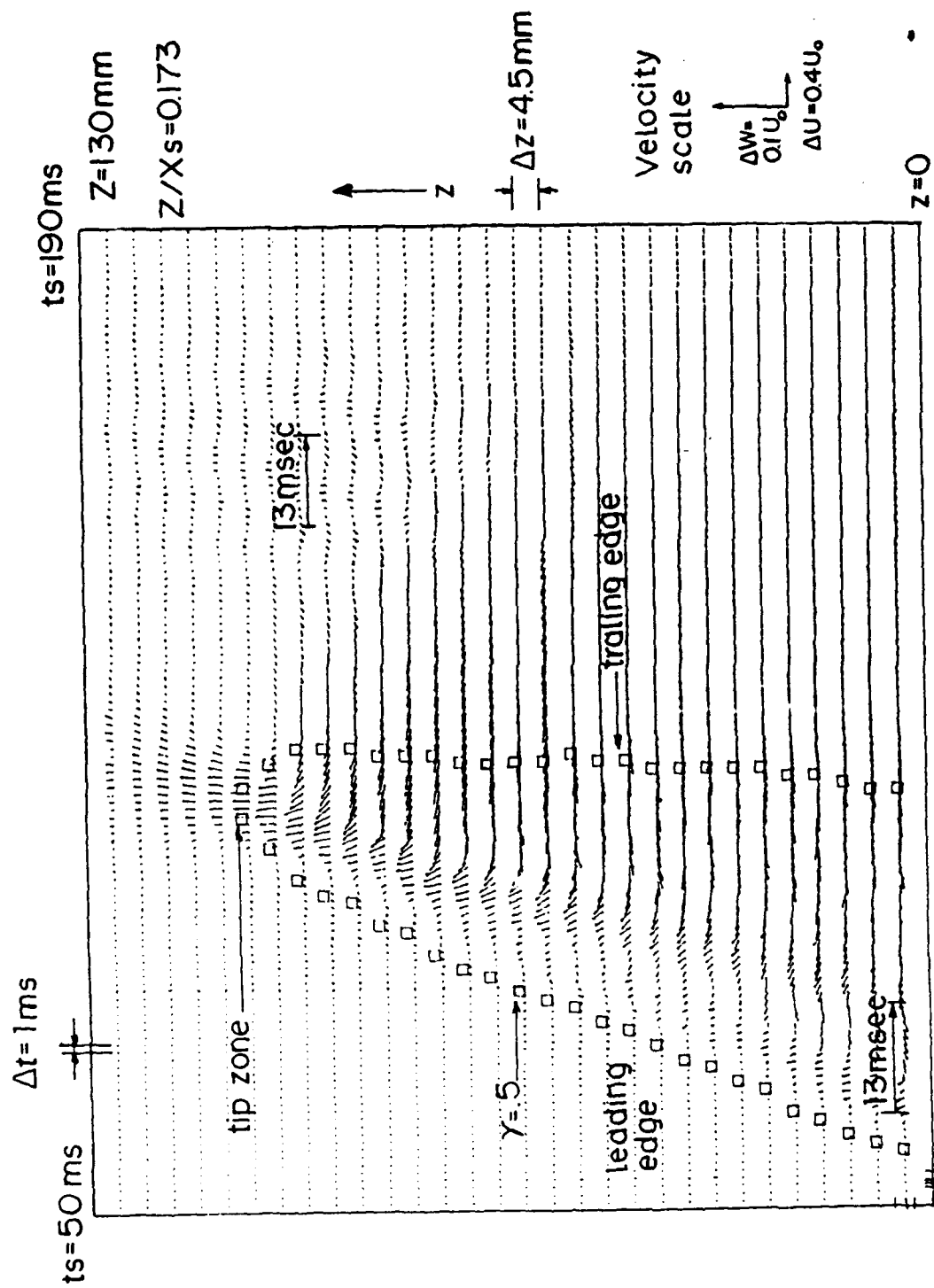


Figure 10

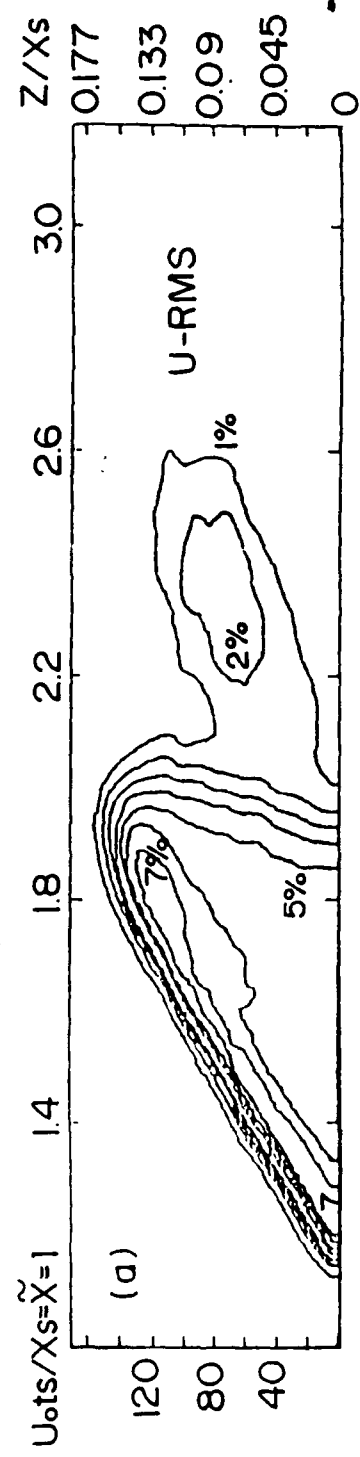
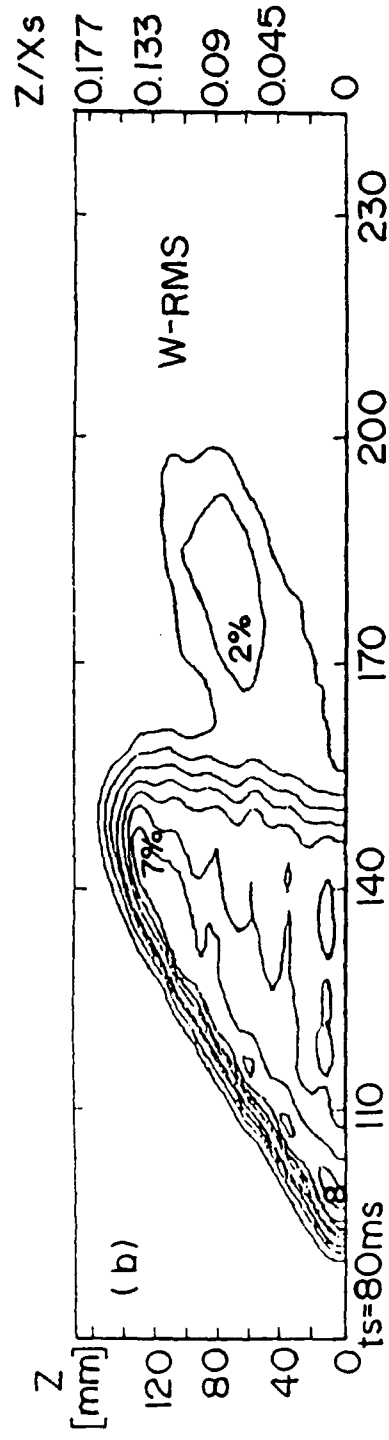


Figure 11

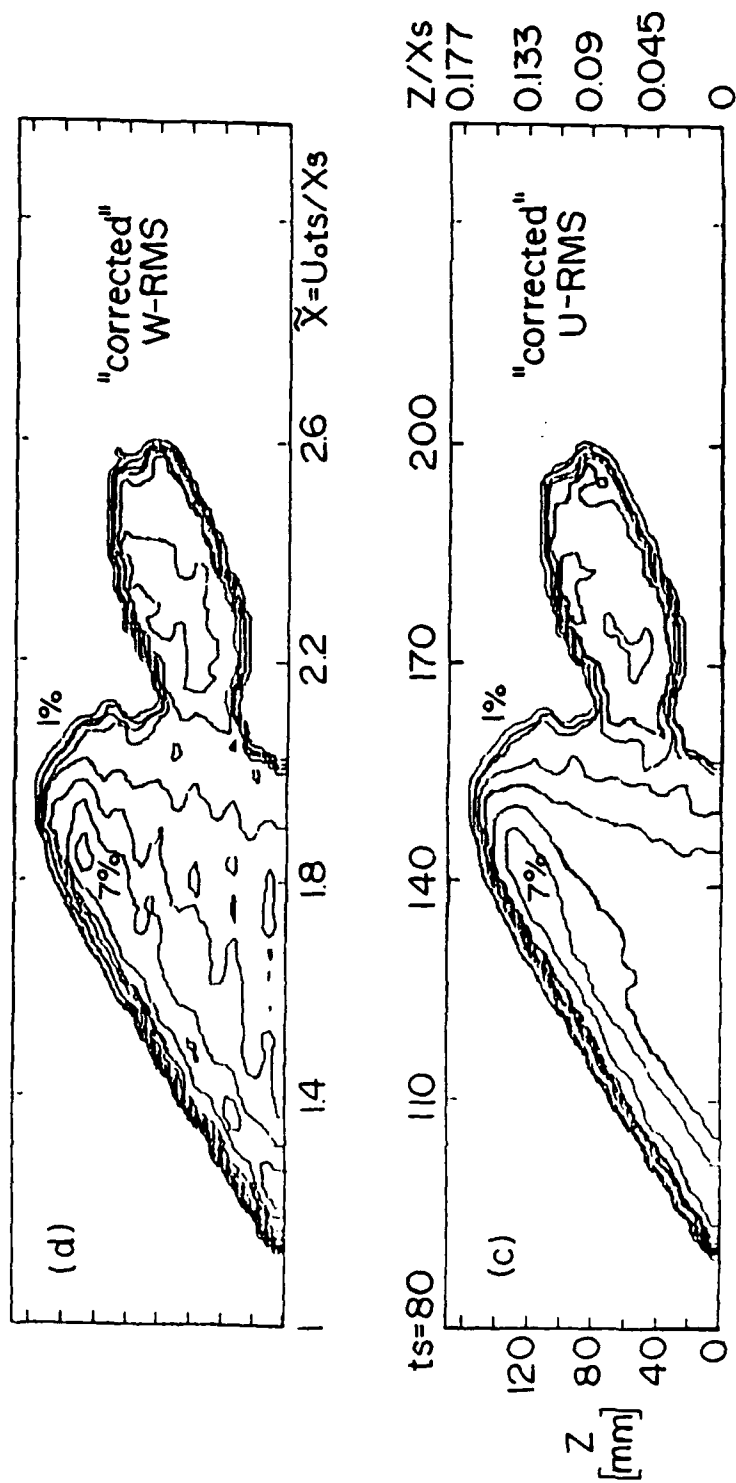


Figure 11

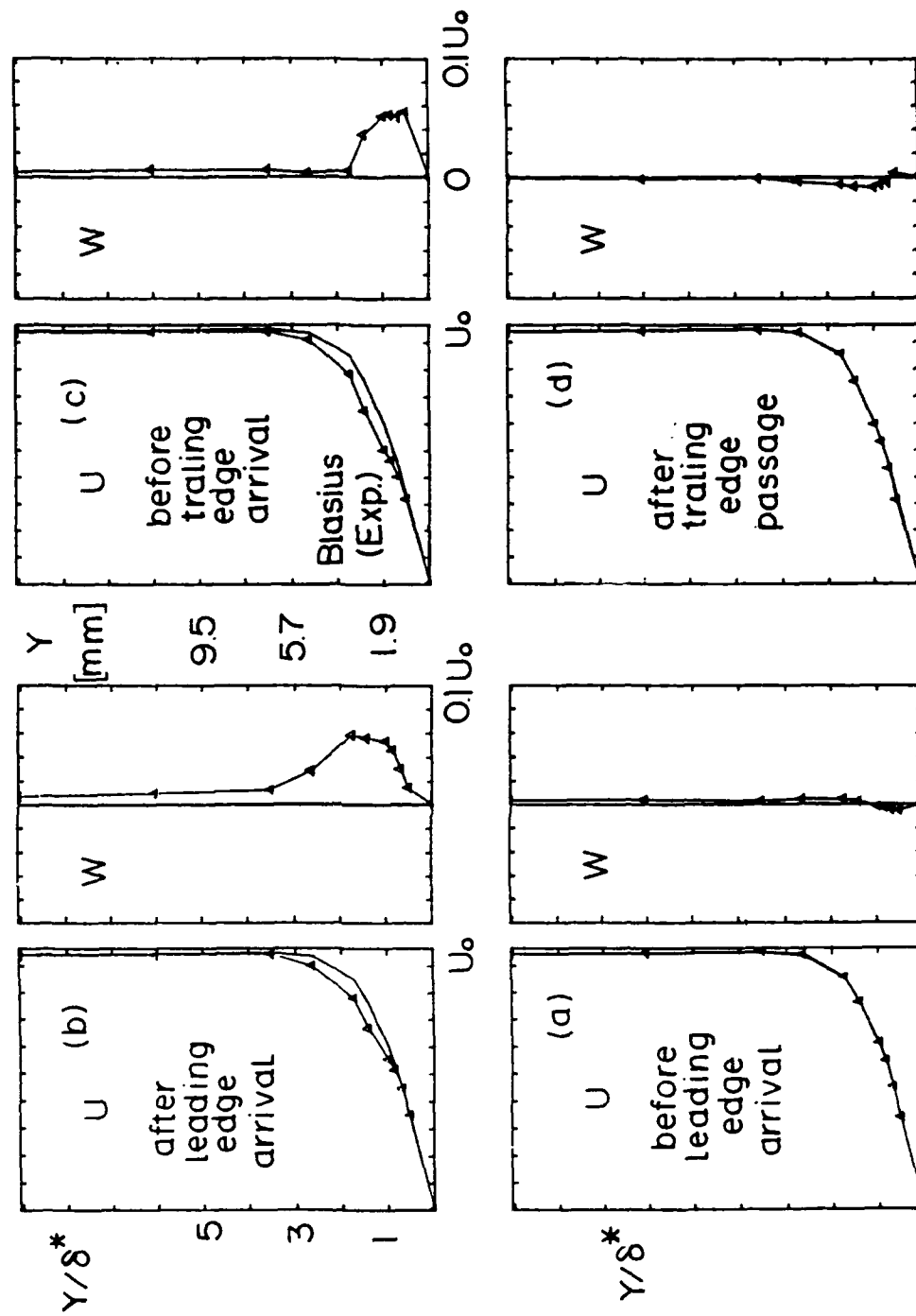


Figure 12